Direct Comparison of A- and T-Strand Minor Groove Interactions in DNA Curvature at A Tracts†

Angèle S. Maki, TaeWoo Kim, and Eric T. Kool*

Department of Chemistry, Stanford University, Stanford, California 94305-5080

Received July 29, 2003; Revised Manuscript Received November 19, 2003

ABSTRACT: To investigate the relative contributions of minor-groove electrostatic interactions in the mechanism of A-tract DNA curvature, we carried out experiments with modified DNA bases in both strands of the tract. We employed 3-deazaadenine nucleoside (D), which lacks the adenine N3 nitrogen in the minor groove and thus cannot act as an electron donor, as well as difluorotoluene (F), a nonpolar thymine mimic. The effects of these analogues in A-tract curvature were quantified using ligation ladder gel mobility methods developed by Crothers and by Maher. Through single substitutions of D in A_5 tracts, we found that this analogue results in decreased curvature only when situated toward the 3′ end of the tract. This is distinct from the behavior in the T-rich strand where F substitution causes the greatest reductions in curvature toward the 5′ end. To test for cooperative pairwise effects, we also studied 10 different D + F double substitutions and found evidence supporting a number of localized cooperative electrostatic interactions but not between the two most sensitive sites in the opposite strands. These results suggest that there are two discrete locations in the A-tract minor groove where electrostatic interactions are important in causing curvature: one near the 5′ end of the T-rich strand, and one near the 3′ end of the A-rich strand. The results are consistent with an important role of localized cations in the minor groove. Possible effects of groove solvation and stacking at the A-tract junction are also discussed.

DNA sequences of four to six consecutive adenines (A tracts), when repeated in phase with a duplex helical repeat, are associated with local helix curvature (*1*). Other properties unique to A tracts are the narrowing of the minor groove toward the 3′ end, the presence of bifurcated hydrogen bonds in the major groove, and the large propeller twist exhibited by the A−T base pairs (*2*−*4*). Although the phenomenon has been studied for over 20 years, the underlying mechanism of A-tract curvature is poorly understood. Models put forward to explain the basis of A-tract curvature fall into two categories: those that rely solely on sequence-dependent base−base interactions and those that take into account the interaction of DNA with its environment. The wedge and junction models fall into the former category, while the hybrid-solvent model falls into the latter. In the wedge model proposed by Trifonov and Sussman, roll angles at ApA steps cause successive adenosines to be nonparallel, as if there were a wedge between the adenines of each step (*5*). The presence of several nonparallel ApA steps phased with the helical repeat of the helix allow the angles to add constructively and cause deflection of the helix axis. In the junction model of Crothers and co-workers, helix curvature is driven by the optimization of stacking at the interface of the highly inclined base pairs of an A tract with normal B-DNA (*6*). The hybrid-solvent model put forward by Williams and co-workers suggests that it is the interaction of specific DNA sequences with water and cations surrounding DNA that results in helix curvature (*7*, *8*). In this model, cations can partition into the minor groove spine of hydration, which itself is coordinated by minor groove functional groups. This partitioning of cations into the groove is dictated by DNA sequence and in particular the functional groups present in the minor groove. In this model, the positive charge of these molecules in the minor groove can neutralize phosphate repulsions and cause helix curvature.

Recent experimental and theoretical evidence lends support to the idea that cations may contribute to A-tract curvature. In separate X-ray crystal structures, Williams and co-workers and Egli and co-workers located Na^+, K^+, Cs^+, Mg^{2+}, Tl^+, and Rb^+ in the minor groove of the Dickerson dodecamer sequence (*7*−*11*). In solution-phase experiments, Hud and Feigon used NMR techniques to localize monovalent and divalent cations in A_{2-5} tracts (*12*−*14*). Using molecular dynamics simulations, Beveridge and co-workers and Wilson and co-workers demonstrated A-tract curvature, and in some cases, minor groove narrowing as a result of either cations partitioning into the minor groove or chemical neutralization of phosphates (*15*−*19*). Maher and co-workers contributed experimental support to the notion that phosphate neutralization can result in DNA curvature through studies with neutral and cationic phosphate analogues (*20*−*23*). Finally, Plavec and Hud have argued for a hybrid explanation for the mechanism of DNA curvature that they call the cation-dependent junction model (*24*). It attempts to explain most of the studies on A tracts to date by combining both the

† Supported by NIH Grant GM52956/EB002059, by a Boehringer Ingelheim Graduate Fellowship to A.S.M., and by a KOSEF fellowship to T.W.K.

* To whom correspondence should be addressed. E-mail: kool@stanford.edu.

10.1021/bi035340m CCC: $27.50
Published on Web 01/07/2004

intrinsic and the extrinsic factors in the mechanism of A-tract curvature. Thus, electrostatic interactions and inherent structural properties were proposed to contribute to the phenomenon.

Investigations into the mechanism of A-tract curvature using DNA base analogues have focused almost entirely on adenine analogues (and thus only on the A-rich strand). McLaughlin and Diekmann explored the role of A-tract bifurcated hydrogen bonds through the substitution of inosine-cytosine (I−C) base pairs for A−T pairs (*25*). Alternating I−C and A−T base pairs prohibits the formation of bifurcated hydrogen bonds. Only modest reductions in DNA curvature resulted from I−C substitution, which suggests that bifurcated bonds are not responsible for A-tract curvature. Seela and Grein probed the role of the minor and major groove hydration in A-tract curvature by removing adenosine's minor and major groove ring nitrogens (N3 and N7) (*26*). Their experiments used A_5 and A_6 tracts polysubstituted with 3- and 7-deazaadenine analogues. Both analogues decreased curvature when substituted toward the 3′ end of the A tract. Systematic monosubstitutions at each position of the A tracts were not carried out; thus, information on site-specific interactions is still lacking. Nielsen and coworkers used a 2,6-diaminopurine (2,6-DAP) analogue of adenine and inosine (I)[1] to investigate the effect of minor-groove width on DNA curvature (*27*). They found that a narrow minor groove is not sufficient to cause DNA curvature and that both analogues had more pronounced effects at the 3′-end.

Recently, we investigated the role of thymine electrostatic interactions in A-tract curvature through substitution with a nonpolar nucleoside isostere, 2,4-difluorotoluene nucleoside (F) (Figure 1A) (*28*). With this nucleotide analogue, the O2 and O4 carbonyl groups of thymine are replaced by much less polar fluorine atoms. This prevents the base from forming electrostatic bonds with water molecules or coordinating cations. Those early data showed that upon substitution with F, the DNA curvature was decreased, but the effect at each position was not uniform. The results supported a contributing role of site-specific electrostatic interactions by the thymine minor groove O2 carbonyl with water and cations. The findings also suggested that major-groove bifurcated hydrogen bonds are not important in A-tract curvature, in agreement with earlier results (*25*, *29*).

Despite the many existing studies on DNA curvature, there is a general lack of experimental data on interactions of the T-rich strand in this phenomenon, and only a few experiments have been published on the removal of minor- or major-groove hydrogen bonding groups from either strand. Furthermore, no data exist yet on the cooperativity of interactions across the two strands in the groove despite the fact that they are widely expected to occur. To address these issues, we now report systematic experiments investigating the role of adenine's electrostatic interactions in the minor groove of the A-rich strand using 3-deazaadenine (D; Figure 1A) to replace A in the A-rich strand of an A_5 tract, with comparison to new data generated with analogue F in the T-rich strand. Using these two analogues both together and separately (Figure 1B), we observed marked effects locally in both strands and found evidence for two separate sites of electrostatic interaction. We also observed pairs of minor groove atoms where cooperative interactions appear to be prominent. The results suggest the presence of two localized cation-binding sites in opposite strands in the minor groove. The implications of the results for solvation, cation binding, and junction models for curvature are discussed.

[1] Abbreviations: D, 3-deazaadenine nucleoside; F, 2,4-difluorotoluene nucleoside; 2,4-DAP, 2,4-diaminopurine; I, inosine.

EXPERIMENTAL PROCEDURES

Synthesis of 3-Deazaa Phosphoramidite. Only the nucleobase has been reported previously (*26*). Thus, we describe the procedural details for the phosphoramidite below.

1H-Imidazo[4,5-c]pyridine (**1**) (*30*). 3,4-Diaminopyridine (5.0 g, 0.046 mol) was vigorously refluxed with HCOOH (10 mL) for 2 h. Excess HCOOH was removed to afford a sticky oil; this was dissolved in ethanol (100 mL) and treated with $CaCO_3$ (ca. 3 g) for 3 h and filtered. The filtrate was concentrated to give 3,4-diformylaminopyridine. 3,4-Diformylaminopyridine (1.3 g) was purified by sublimation in vacuo ($bp_{5\sim6}$ 140∼150 °C) to afford **1** (0.71 g, 6.0 mmol, 13%) as a white crystal. ^{1}H NMR (DMSO-d_6, ppm) 8.93 (s, 1H), 8.32 (s, 1H), 8.30 (d, 1H, J = 5.6 Hz), 7.59 (d, 1H, J = 5.6 Hz); LR MS (ESI+) mass calcd 120.06 for [$C_6H_5N_3$ + H], found 120.1 (100%).

1H-Imidazo[4,5-c]pyridine 5-oxide (**2**) (*30*). Compound **1** (0.71 g, 6.0 mmol) was dissolved in H_2O_2 (2 mL, 30 wt. %) and glacial AcOH (20 mL), and the reaction mixture was stirred at 60 °C. After 1 day, an additional aliquot of H_2O_2 (30%, 1 mL) was injected, and the mixture was stirred for 2 days at 60 °C. Excess H_2O_2 and AcOH were removed in vacuo to afford a residue. Flash chromatography of the residue (silica gel, CH_2Cl_2/MeOH/ammonia water, 10:1:0.1 to 5:1: 0.5) produced **2** (0.54 g, 4.0 mmol, 68%) as a solid. ^{1}H NMR (DMSO-d_6, ppm) 12.5 (br, 1H), 8.66 (s, 1H), 8.43 (s, 1H), 8.02 (d, 1H, J = 14 Hz), 7.62 (d, 1H, J = 14 Hz).

4-Chloro-1H-imidazo[4,5-c]pyridine (**3**) (*30*). A suspension of **2** (0.54 g, 4.0 mmol) in $POCl_3$ (130 mL) was refluxed for 4 h until the oxide was completely dissolved. Excess $POCl_3$ was removed in vacuo to afford a residue. To this was added water (5 mL), and the mixture was neutralized with aqueous ammonia and concentrated in vacuo. The residue was dissolved in 1-butanol (70 mL), and the organic layer was washed with water (20 mL × 3) and concentrated in vacuo. Flash chromatography of the residue (silica gel, CH_2Cl_2 to CH_2Cl_2/MeOH, 95:5) produced **3** (0.44 g, 2.9 mmol, 72%) as a white solid. ^{1}H NMR (DMSO-d_6, ppm) 8.48 (s, 1H), 8.12 (d, 1H, J = 10.8 Hz), 7.62 (d, 1H, J = 11.6 Hz); LR MS (ESI+) mass calcd 176.0 for [$C_6H_4N_3{}^{35}Cl$ + Na], found 176.1 (100%), 178.0 for [$C_6H_4N_3{}^{37}Cl$ + Na], found 178.1 (30%).

*4-Chloro-1-[2′-deoxy-3′,5′-di-O-(4-toluoyl)-β-*D*-erythro-pentofuranosyl]-1H-imidazo[4,5-c]pyridine* (**5**) (*31*). A suspension of KOH (0.40 g, 7.1 mmol) and TDA-1 (tris[2-(2-methoxyethoxy)ethyl]amine, 100 μL) in acetonitrile (100 mL) was stirred for 5 min at room temperature. Then **3** (0.44 g, 2.9 mmol) was dissolved therein under warming (80 °C). The solution was brought to 40 °C, and 1′-chloro-1′, 2′-dideoxy-3′,5′-di-*O*-toluoyl-α-D-ribofuranose (**4**) (*32*) (1.23 g, 3.2 mmol) was added portionwise under stirring. The mixture was held at 40 °C for 15 min, then filtered over Celite 545 and concentrated in vacuo. Flash chromatography

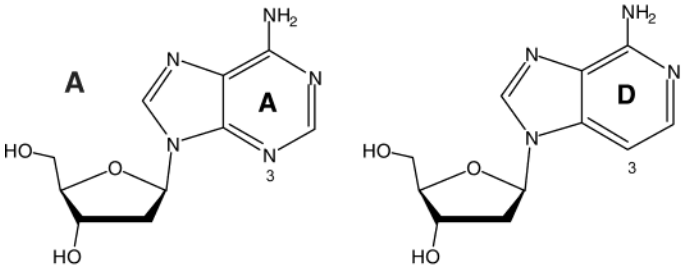

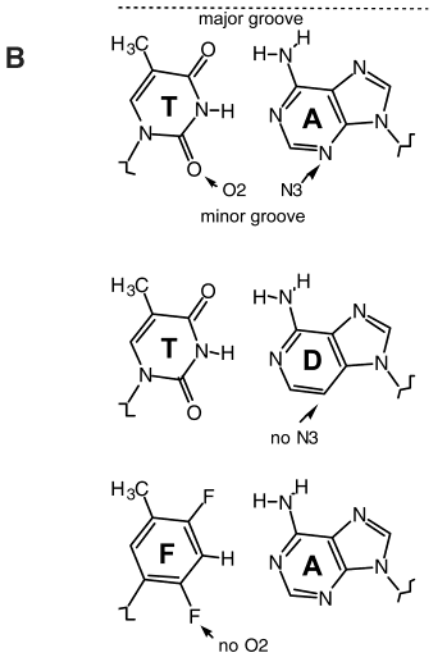

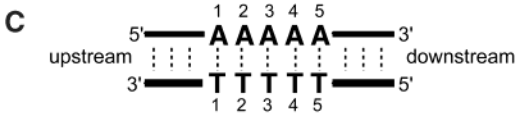

D

Curvature standard duplex
5'-GAAAAACGCCGCGCCGCCGCC
GGCTTTTTGCGGCGCGGCGGC-5'

D1-substituted *cis* duplex
5'-GAAAAACGCCGCDAAAACGCC
GGCTTTTTGCGGCGTTTTTGC-5'

D1-substituted *ortho* duplex
5'-GAAAAACGCCDAAAAGCCGCC
GGCTTTTTGCGGTTTTTCGGC-5'

D1-substituted *trans* duplex
5'-GAAAAACGDAAAACCGCCGCC
GGCTTTTTGCTTTTTGGCGGC-5'

D2-substituted *cis* duplex
5'-GAAAAACGCCGCADAAACGCC
GGCTTTTTGCGGCGTTTTTGC-5'

D2-substituted *ortho* duplex
5'-GAAAAACGCCADAAAGCCGCC
GGCTTTTTGCGGTTTTTCGGC-5'

D2-substituted *trans* duplex
5'-GAAAAACGADAAACCGCCGCC
GGCTTTTTGCTTTTTGGCGGC-5'

D3-substituted *cis* duplex
5'-GAAAAACGCCGCAADAACGCC
GGCTTTTTGCGGCGTTTTTGC-5'

D3-substituted *ortho* duplex
5'-GAAAAACGCCAADAAGCCGCC
GGCTTTTTGCGGTTTTTCGGC-5'

D3-substituted *trans* duplex
5'-GAAAAACGAADAACCGCCGCC
GGCTTTTTGCTTTTTGGCGGC-5'

D4-substituted *cis* duplex
5'-GAAAAACGCCGCAAADACGCC
GGCTTTTTGCGGCGTTTTTGC-5'

D4-substituted *ortho* duplex
5'-GAAAAACGCCAAADAGCCGCC
GGCTTTTTGCGGTTTTTCGGC-5'

D4-substituted *trans* duplex
5'-GAAAAACGAAADACCGCCGCC
GGCTTTTTGCTTTTTGGCGGC-5'

D5-substituted *cis* duplex
5'-GAAAAACGCCGCAAAADCGCC
GGCTTTTTGCGGCGTTTTTGC-5'

D5-substituted *ortho* duplex
5'-GAAAAACGCCAAAADGCCGCC
GGCTTTTTGCGGTTTTTCGGC-5'

D5-substituted *trans* duplex
5'-GAAAAACGAAADCCGCCGCC
GGCTTTTTGCTTTTTGGCGGC-5'

D3F1-substituted *cis* duplex
5'-GAAAAACGCCGCAADAACGCC
GGCTTTTTGCGGCGFTTTTGC-5'

D3F1-substituted *ortho* duplex
5'-GAAAAACGCCAADAAGCCGCC
GGCTTTTTGCGGTTTTTCGGC-5'

D3F1-substituted *trans* duplex
5'-GAAAAACGAADAACCGCCGCC
GGCTTTTTGCFTTTTGGCGGC-5'

D3F2-substituted *cis* duplex
5'-GAAAAACGCCGCAADAACGCC
GGCTTTTTGCGGCGTFTTTGC-5'

D3F2-substituted *ortho* duplex
5'-GAAAAACGCCAADAAGCCGCC
GGCTTTTTGCGGTFTTTCGGC-5'

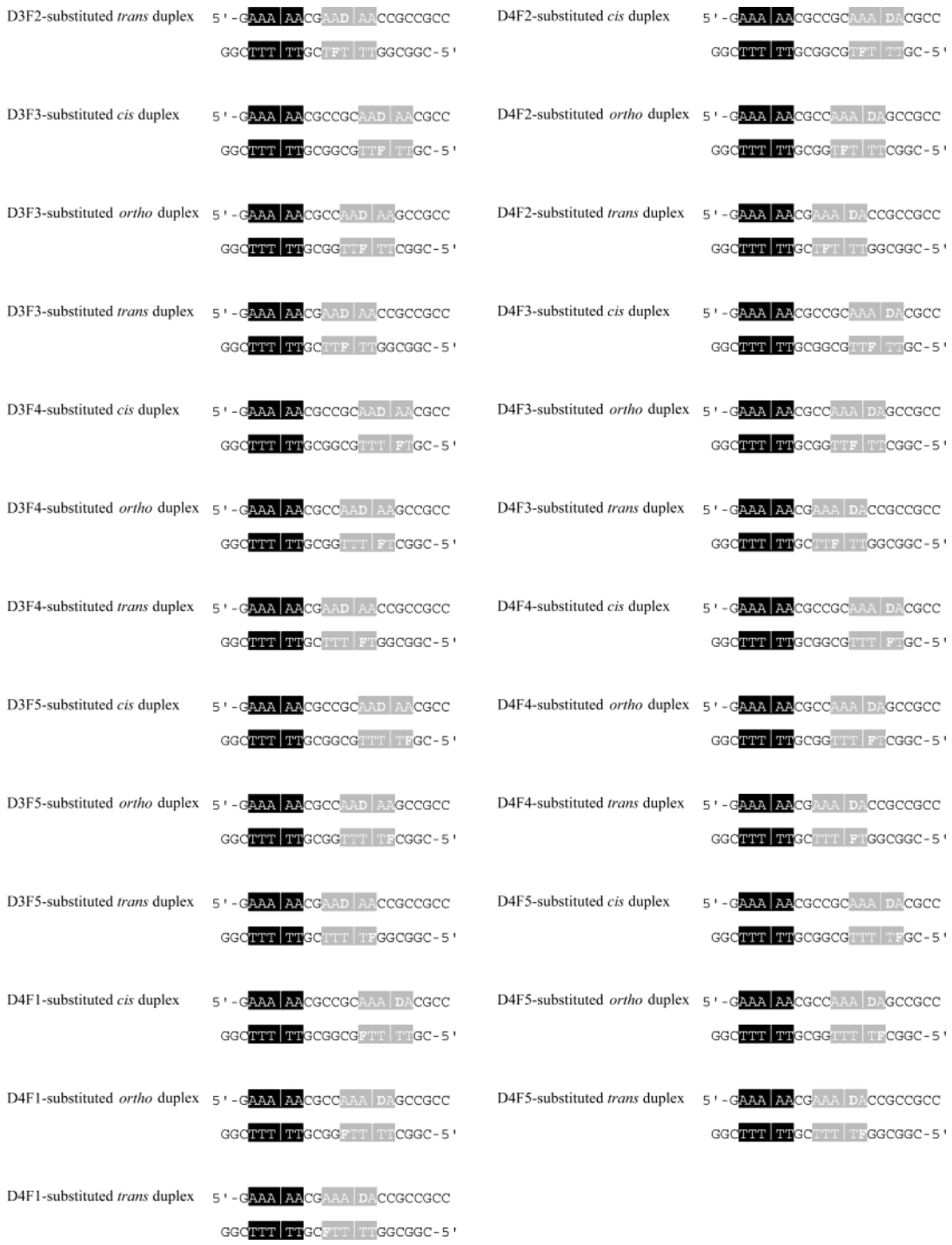

FIGURE 1: (A) Structures of adenine (A), 3-deazaadenine (D), thymine (T), and difluorotoluene (F) as their deoxynucleoside derivatives. (B) Representations of A−T, D−T, and D−F base pairs indicating which groups have been modified with respect to groove orientation. (C) Diagram of the A-tract showing position numbering. (D) DNA duplex sequences used in this study. The A tract in the black box represents the internal reference A tract, while the A tract in gray represents the test A tract. The vertical line within each of the boxes is the assigned center of curvature.

of the residue (silica gel, CH_2Cl_2/MeOH, 100:1) produced the regioisomeric mixture (N^1/N^3-glycosides) as a colorless oil. The major product **5** (0.46 g, 0.92 mmol, 32%) crystallized from a small volume of ethyl acetate (4 mL)/cyclohexane (4 mL) upon cooling. ^{1}H NMR ($CDCl_3$, ppm) 8.73 (s, 1H), 8.07 (d, 1H, J = 5.6 Hz), 7.98 (d, 2H, J = 8.0 Hz), 7.84 (d, 1H, J = 5.8 Hz), 7.79 (d, 2H, J = 8.2 Hz), 7.39 (d, 2H, J = 7.8 Hz), 7.30 (d, 2H, J = 8.0 Hz), 6.63 (app t, 1H, J = 4.5 Hz), 5.72 (m, 1H), 4.5−4.7 (m, 3H), 3.2−3.05 (m, 1H), 3.0−2.8 (m, 1H), 2.50 (s, 6H).

*4-Chloro-1-(2′-deoxy-β-*D*-erythro-pentofuranosyl)-1H-imidazo[4,5-c]pyridine* (**6**) (*31*). To a solution of **5** (0.46 g, 0.91 mmol) in methanol (10 mL) was added sodium methoxide (0.52 g, 25 wt. % solution in methanol), and the reaction mixture was stirred at room temperature for 12 h. The solution was neutralized with aqueous NH_4Cl and concentrated in vacuo. Flash chromatography of the residue (silica gel, CH_2Cl_2/MeOH, 10:1 to CH_2Cl_2/MeOH/ammonia water 100:15:1) produced **6** (0.24 g, 0.89 mmol, 98%) as a solid. ^{1}H NMR (DMSO-d_6, ppm) 8.71 (s, 1H), 8.16 (d, 1H, J =

5.6 Hz), 7.87 (d, 1H, $J = 5.8$ Hz), 6.41 (app t, 1H, $J = 4.5$ Hz), 5.38 (m, 1H), 5.03 (m, 1H), 4.40 (m, 1H), 3.89 (m, 1H), 3.56 (m, 2H), 2.6−2.3 (m, 2H).

*4-Amino-1-(2′-deoxy-β-*D*-erythro-pentofuranosyl)-1H-imidazo[4,5-c]pyridine* (**7**) (*33*). Compound **6** (0.24 g, 0.89 mmol) was dissolved in hydrazine hydrate (25 mL) and the solution was refluxed for 90 min. Excess hydrazine was removed in vacuo and the residue was coevaporated with ethanol (2 × 30 mL) and then ethanol/toluene (2 × 30 mL), and then dissolved in ethanol (25 mL). After addition of Raney nickel (2 g, Raney 2800 nickel, slurry in water), the suspension was stirred under reflux for 2 h. The catalyst was filtered off, washed with ethanol and the combined filtrates were evaporated to give a dark residue. Flash chromatography of the residue (silica gel, CH_2Cl_2: MeOH, 10:1 to CH_2Cl_2: MeOH: ammonia water 100: 10:2) produced **7** (72 mg, 0.29 mmol, 33%) as a solid. ^{1}H NMR (DMSO-d_6, ppm) 8.37 (s, 1H), 7.67 (d, 2H, $J = 6.0$ Hz), 6.98 (d, 2H, $J = 6.0$ Hz), 6.61 (br, 2H), 6.27 (app t, 1H, $J = 6.6$ Hz), 5.36 (m, 1H), 4.98 (m, 1H), 4.37 (m, 1H), 3.86 (m,1H), 3.55 (m, 2H), 2.6−2.3 (m, 2H).

*4-(Benzoylamino)-1-(2′-deoxy-β-*D*-erythro-pentofuranosyl)-1H-imidazo[4,5-c]pyridine* (**8**) (*26*). Compound **7** (72 mg, 0.29 mmol) was dried by coevaporation with anhydrous pyridine, dissolved in pyridine (3 mL), and treated with Me_3-SiCl (0.20 mL, 1.6 mmol) under stirring at room temperature. After 30 min, benzoyl chloride (44 μL, 0.38 mmol) was injected, and the mixture was stirred for 3 h. The mixture was quenched with water (1 mL) and neutralized by ammonia water (2 mL, 10 to ∼35% ammonia). The solution was concentrated in vacuo, and flash chromatography of the residue (silica gel, CH_2Cl_2/MeOH, 4:1) produced **8** (75 mg, 0.21 mmol, 72%). ^{1}H NMR (DMSO-d_6, ppm) 8.64 (s, 1H), 8.07 (d, 1H, $J = 5.6$ Hz), 7.79−7.38 (m, 6H), 6.41 (app t, 1H, $J = 7.2$ Hz), 5.38 (m, 1H), 5.03 (m, 1H), 4.39 (m, 1H), 3.88 (m, 1H), 3.56 (m, 2H), 2.6−2.35 (m, 2H).

*4-(Benzoylamino)-1-[2′-deoxy-5′-O-(dimethoxytrityl)-β-*D*-erythro-pentofuranosyl]-1H-imidazo[4,5-c]pyridine* (**9**) (*26*). Compound **8** (0.29 g, 0.82 mmol) was dried by coevaporation with anhydrous pyridine and dissolved in pyridine (10 mL). DMTCl (4,4-dimethoxytriphenylmethyl chloride, 0.41 g, 1.2 mmol) was added to the solution at 0 °C. The reaction mixture was stirred for 12 h at room temperature. The reaction mixture was partitioned into 5% aqueous $NaHCO_3$-ethyl acetate, and the organic layer was washed with 5% aqueous $NaHCO_3$ (× 2) brine. The solution was dried over anhydrous Na_2SO_4 and concentrated in vacuo. Flash chromatography of the residue (silica gel, hexane/ethyl acetate, 1:2 to ethyl acetate) produced **9** (0.27 g, 0.41 mmol, 50%) as a pale yellow solid. ^{1}H NMR ($CDCl_3$, ppm) 8.01 (s, 1H), 7.90 (d, 1H, $J = 5.6$ Hz), 7.80 (d, 2H, $J = 7.0$ Hz), 7.37−7.14 (m, 13H), 6.75 (dd, 4H, $J = 8.8$, 2.8 Hz), 6.12 (app t, 1H, $J = 7.0$ Hz), 4.54 (m, 1H), 4.07 (m, 1H), 3.71 (s, 6H, -OCH_3), 3.30 (m, 3H), 2.5−2.4 (m, 1H), 2.37−2.3 (m, 1H).

*4-(Benzoylamino)-1-[2′-deoxy-5′-O-(dimethoxytrityl)-3′-O-(2-cyanoethyl N,N-*diisopropylphosphoramidite*)-β-*D*-erythro-pentofuranosyl]-1H-imidazo[4,5-c]pyridine* (**10**). The 5′-*O*-DMT compound **9** (0.27 g, 0.41 mmol) was dissolved in dry dichloromethane (10 mL) and to this were added DIPEA (diisopropylethylamine, 0.30 mL, 1.7 mmol) and 2-cyanoethyl *N,N*-diisopropylchlorophosphoramidite (140 μL, 6.2 mmol). The reaction mixture was stirred at room temperature for 5 h and concentrated in vacuo. Flash chromatography of the residue (silica gel, hexane/ethyl acetate/triethylamine, 10:10:1) produced **10** (285 mg, 0.33 mmol, 81%) as a white foam. ^{1}H NMR ($CDCl_3$, ppm) 8.13 (m, 1H), 7.96−7.80 (m, 1H), 7.81 (d, 2H, $J = 7.4$ Hz), 7.48−7.15 (m, 13H), 6.79−6.72 (m, 4H), 6.3 (m, 1H), 4.4−4.1 (m, 3H), 3.72 (s, 6H), 3.6−3.3 (m, 5H), 2.75−2.44 (m, 4H), 1.28−1.07 (m, 12H).

Curvature Measurements. The ligation ladder method of Maher and co-workers was used to quantify the effects of nucleotide analogue substitutions on A_5-tract curvature (*34*). This approach for quantifying DNA curvature relies on the fact that progressively longer multimers of phased A tracts exhibit greater gel mobility anomalies (*34*, *35*). A duplex representing two helical turns and containing two A_5 tracts is used (Figure 1D). One A tract acts as an internal reference with a known curvature angle and direction (A tract in the black box), while the other A tract serves as a test tract (A tract in the gray box). Modifications to the sequence can be made in the test A tract to evaluate their effect(s) on curvature magnitude and direction relative to the reference A tract. In the study reported here, F was substituted for T, and D was substituted for A, systematically at each possible position in the test tract. All duplexes have 3′ extensions that permit ligation to occur at the appropriate end of another duplex, ensuring proper phasing of the A tracts. Thus, the number of A tracts in one duplex increases upon ligation, causing these longer duplexes to exhibit greater curvature and have a larger mobility anomaly. The relationship between electrophoretic mobility, helix curvature, and number of A tracts is used to determine the curvature angle and apparent orientation (e.g., toward the minor groove).

For each analogue substitution, three duplexes (cis, ortho, and trans) are needed to determine curvature direction. These three duplexes differ by the relative phasing of their A tracts. In the cis case, the A tracts are separated by one complete turn of the helix and thus occur on same face of the helix. This produces the greatest net curvature and largest mobility anomaly. In the trans case, the A tracts are separated by a half-turn of the helix. This results in two bends in opposite directions and little to no net curvature or gel mobility anomaly. In the ortho duplex, the A tracts are separated by about three-quarters of a turn; thus, the bends are slightly offset. In this situation, the angles are not completely additive nor do they do they cancel each other out. These three different phasings allow determination of the overall duplex curvature direction, which depends on both the location and the direction of the individual curvature sites.

The position and orientation of the curvature in the test A tract is evaluated by the spacing correction, D. This parameter is a measure of the difference (in bp) between the test A tract's actual center of curvature and its assigned center (indicated by the vertical line between A3 and A4 of the test A tract as shown in Figure 1D). If D is zero, then the actual center of curvature is at the same position as the assigned center of curvature, and curvature is toward the minor groove of the A tract.

Monosubstitution with 3-deazaadenosine (D) was carried out at each of the five possible positions of the test A tract as shown in Figure 1C,D. Disubstitutions with D and F were carried out in a similar fashion, with both analogues in the test A or T tracts. In these disubstitutions, F was substituted at each of the five possible positions of the T tract with

Table 1: A-Tract Curvature Angles and Positions for D- and D,F-substitutions

substitution	curvature angle (deg)[a]	curvature position
D1	20.2 ± 0.4	−0.049 ± 0.06
D2	19.1 ± 1.6	−0.009 ± 0.01
D3	16.1 ± 1.1	0
D4	11.9 ± 0.4	−0.25 ± 0.02
D5	13.5 ± 0.3	−0.44 ± 0.03
D3,F1	12.8 ± 0.5	1.4 ± 0.03
D3,F2	5.7 ± 0.4	−1.4 ± 0.1
D3,F3	*b*	−0.60 ± 0
D3,F4	12.7[c]	−1.9
D3,F5	13.3 ± 1.4	−0.29 ± 0.05
D4,F1	11.8 ±0.3	1.6 ± 0.02
D4,F2	3.9 ± 0.1	−1.4 ± 0.4
D4,F3	8.6 ± 0.3	−1.4 ± 0.05
D4,F4	11.2 ± 0.6	−1.4 ± 0.06
D4,F5	12.2 ±0.5	−0.032 ± 0.02

[a] Average value ± standard deviation based on at least three separate experiments unless otherwise indicated. [b] Unable to fit data and obtain curvature angles. [c] Data from one value; others gave poor fits.

concomitant substitution of D at either position 3 or 4 of the A tract, the most perturbing positions for substitution with D (Figure 1C). Data analysis was carried out as detailed previously (*28*, *34*). All curvature data are the result of at least three sets of experiments, and averages are shown with standard deviations. Two exceptions were noted. Curvature results for disubstitution at D3F3 were not obtained as proper fitting of the data was not possible. Disubstitution at position D3F4 yielded only one result as fitting of the data from several other trials was also not possible.

RESULTS

To compare minor groove effects of the A-rich strand and T-rich strand on DNA curvature, we used two hydrogen-bonding-deficient DNA base analogues (Figure 1A,B). 3-Deazaadenine (D) was used in the A-rich strand to remove single H-bonding groups in the minor groove, and difluorotoluene (F) was used as a nonpolar, non-hydrogen bonding replacement for T in the T-rich strand (Figure 1A,B). To use Maher's ligation ladder approach to quantify A-tract curvature (*34*), an accurate value of the helical repeat must be known for helices containing these analogues. We previously showed that single F substitution did not alter the helical repeat unit from that of T-substituted DNA (*28*). However, this had not been determined for analogue D. Thus, we carried out experiments to measure the helical repeat for duplexes containing D and found the value to be equal to 10.4 bp/helical turn for a D3-substituted A_5-tract (see Supporting Information), the same as unmodified DNA. For subsequent experiments, we assumed that the helical repeat would be the same for other D-monsubstituted duplexes and used the sequence contexts described previously (Figure 1D) (*34*).

We analyzed five sets of data resulting from the systematic monosubstitution of D into an A_5 tract. When D was substituted at the A1 and A2 positions (numbered from the 5′ end of the A-rich strand; Figure 1C), the duplexes displayed gel mobility anomalies similar to the unsubstituted A-tract duplexes (Figure 2A). However, we observed increases in mobility upon substitution of D at positions A3−A5, with the largest increase occurring with the D4 substitution (Figure 2B). Calculations of curvature confirmed that monosubstitution of D in the A_5 tract had no effect at the 5′ end, while it decreased DNA curvature when substituted near the 3′ end of the tract (Table 1). The greatest reduction in curvature, to 13.0° from the original 19.0° for an unmodified A tract, occurred at the A4 position.

Electrostatic interactions in the groove, such as those involving waters of solvation or bound cations, might be expected to make multiple contacts simultaneously. Indeed, X-ray structures commonly show water molecules and cations bridging groups across the two strands (*8*, *36*). To investigate possible cooperative interactions, we carried out 10 double substitutions with D and F in addition to the above single substitutions. In the first set of five disubstitutions, A3 was replaced by D, and T1−T5 were individually substituted with F. In the second set, D was substituted for A4 and F was replaced each of T1-T5. We chose to substitute A at positions 3 and 4 since these positions showed the greatest change in curvature in the monosubstitution experiments. Analysis of curvature in these 10 cases revealed that disubstitution increased mobility of the duplexes in all 10 (Table 1). The largest change occurred with the D4F2 double substitution (Figure 3), which resulted in a decrease of curvature from 19.0 to 3.9°.

The position and orientation of the curvature in the test A tract was evaluated by the spacing correction, D. Previously, we found that the unsubstituted A-tract duplex has a negligible D value of 0.20 (*28*). Since D is almost zero in this case, it indicates that the assigned center of curvature coincides with the actual center or curvature and that curvature is toward the minor groove of the A tract. The D values for the D-substituted and the D,F-substituted A-tract duplexes are all equal to or less than 1.9 bp, establishing that they are curved toward the minor groove as well. The centers of curvature may be shifted by 1−2 bp in the cases where D is 1−1.9 or the orientation of the curvature is different by up to ±65° (i.e., 1.9 bp × 360°/10.5 bp) from the perfect cis orientation (relative to the reference tract).

DISCUSSION

In this paper, we have applied Maher's refinement of Crothers' ligation ladder approach to quantify the effects of minor groove modification on A-tract DNA curvature. The ligation ladder approach is a well-established gel mobility-based technique that has proven useful in multiple laboratories for testing the effect of nucleotide modification in A tracts (*34*). It is conceivable that altered electrostatic effects on gel mobility during electrophoresis might cause artifacts in such measurements, whereas solution-phase measurements such as cyclization assays may avoid this (*37*). However, there are drawbacks to the cyclization approach as well (*38*). In the present case, we are most interested in relative rather than absolute curvatures, and each gel analysis in the ligation ladder approach is calibrated to a standard duplex containing an unmodified A-tract. Indeed, Maher and co-workers used this method to improve upon the cyclization assay analysis (*38*). Thus, we believe it is reasonable in the present case to use the ligation ladder method to assess the relative effects of nucleotide modification on A-tract curvature.

The present data show that removal of a single hydrogen bond acceptor (the N3 nitrogen of adenine) in the A-rich strand of an A_5 tract generally decreased curvature and had

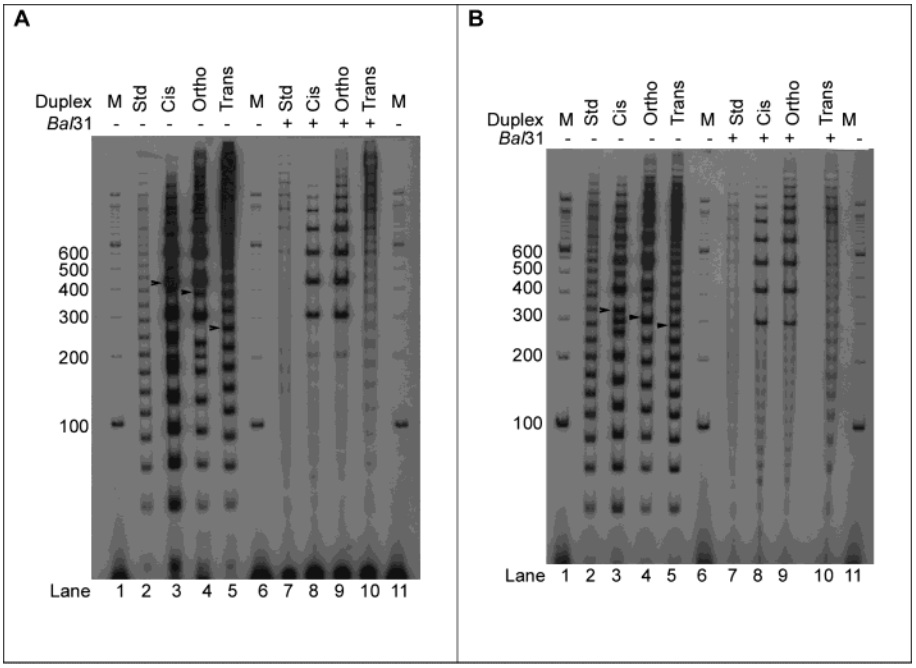

FIGURE 2: Autoradiograms of D1-substituted (A) and D4-substituted (B) A-tract ligation ladders. Autoradiogram of the unsubstituted A-tract ligation ladder can be found in ref *28*. M corresponds to the 100-bp DNA ladder. Lanes 2−5 represent ligation ladders not subjected to nuclease digestion, while lanes 7−10 represent these same ligation ladders digested with *Bal*31. The arrowheads point to the ligated nonamer illustrating mobility differences among the duplexes. The bands in lanes 7−10 correspond to DNA circles formed during the ligation. These bands must be identified so they can be ignored in the data analysis.

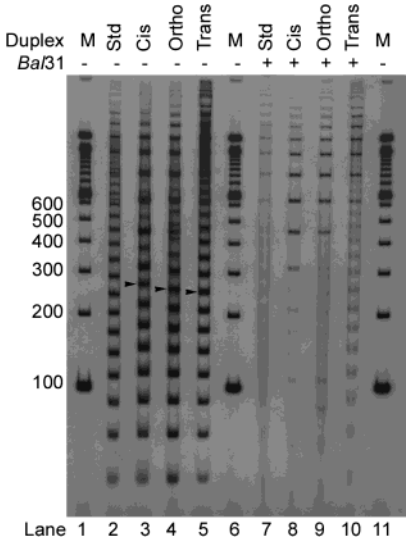

FIGURE 3: Autoradiogram of D4F2-substituted A-tract ligation ladders. M corresponds to the 100-bp DNA ladder. Lanes 2−5 represent ligation ladders not subjected to nuclease digestion, while lanes 7−10 represent these same ligation ladders digested with *Bal*31. The arrowheads point to ligated nonamer illustrating mobility differences among the duplexes.

the greatest effect near the 3′ end of the A tract. This is consistent with the results of Seela and Grein, who found that polysubstitution of 3-deazaadenosine analogues reduced curvature when substituted into the 3′ end of A_{5-6} tracts (*26*). They argued that because the A-tract duplexes lacking the minor groove nitrogens at the 5′ end have very similar mobilities to unmodified A-tract duplexes, the spine of hydration in the minor groove must not be an important factor in curvature. The current results may support this conclusion. The spine of hydration clearly involves waters bridging both T and A residues along the entire length of the groove.

Table 2: Comparison of Curvature Angles from Monosubstitutions and Disubstitutions

substitution position	D (deg)	F [a] (deg)	D3F (deg)	D4F (deg)
1	20.2	12.7	12.8	11.8
2	19.1	5.29	5.70	3.91
3	16.1	9.64	*b*	8.58
4	11.9	13.8	12.7[c]	11.2
5	13.5	17.9	23.3	12.2

[a] Values from ref *28*. [b] Unable to fit data and obtain curvature angles. [c] Data from one value; others gave poor fits.

However, we see asymmetric effects where interactions with T (and not A) residues at the 5′ end of the tract are important, and interactions with A residues (and not T) at the 3′ end are important. Thus, our data are most consistent with two fairly localized electrostatic effects in opposite strands and at opposite ends of the A tract causing the curvature.

Notably, a direct comparison of the magnitudes of the decreases in curvature for the two strands shows that substitutions in the T-rich strand had the more pronounced effect (Table 2). This is consistent with the importance of direct electrostatic interactions (i.e., bound waters or metal ions) at O2 and N3 atoms in the floor of the groove. Since O2 has the greater electron density and greater polarizability, it is expected to make stronger interactions with electron-deficient species. However, one should note that the analogue F is different from D in that both minor groove and major groove hydrogen bonding groups are missing, whereas with D the major groove is unchanged. Thus, we cannot rule out major groove electrostatic effects with the former analogue.

What is perhaps most intriguing about the effects of removal of the minor-groove hydrogen bonding groups in both A- and T-rich strands is the fact that they reveal two separate sites of possible interaction at opposite ends of the

tract. Substitutions in the T-rich strand had the most pronounced effect at the 5′ end of the A tract, while substitutions in the A-rich strand had the greatest impact at the 3′ end. Thus, our results are consistent with two separate interactions, as opposed to a single cooperative interaction spanning A and T residues across the groove. The A-strand effects are most pronounced at A4 and A5, while the T-strand effects are concentrated at T2 and T3. These two locations are at relatively remote positions (in spatial distance) in the tract. For example, the A4 nitrogen is ca. 5.5 Å from the T2 oxygen, likely too distant to be easily explained by single water molecules cooperatively bound between these positions. The T2−A5 oxygen to nitrogen distance is even greater, ∼9.3 Å.

Our double substitution experiments add insight into the possibility of cooperative interactions between DNA bases from both strands of the duplex. Disubstitution decreases curvature angles, but the reduction achieved by any given disubstitution was in most cases essentially the same as that obtained from the corresponding monosubstitution that had the greatest effect (Table 2). With the D4F4 disubstitution, for example, the curvature angle was 11.2°. The corresponding D4 and F4 monosubstitutions yielded curvature angles of 11.9 and 13.8°, respectively; thus, the disubstitution result seems to be equivalent to that from the D4 monosubstitution. Similarly, with the D3F1 disubstitution, the curvature angle is similar to the F1 monosubstitution. This suggests the existence of local cooperative interactions spanning the groove between nearby A and T minor groove residues, where removal of even one interacting group of a pair removes the full contribution to curvature from that region. Interestingly, with double substitutions more remote from one another, as in the D4F2 substitution (distance ∼5.5 Å), we observe less cooperativity. In this disubstitution, both of the most sensitive locations contain analogues, and there does appear to be a synergistic increase in the effect on curvature. Thus, overall the double substitution results are most consistent with local cooperativity, but not cooperativity between the two most sensitive sites that are found at opposite ends of the A tract, being a factor in A-tract curvature.

It appears that there is no direct relationship between duplex stability and curvature, a finding that validates the use of our analogues to probe the curvature mechanism. F substitution into short duplexes has been found to be significantly destabilizing (*39*), yet it only affects curvature at certain positions and not all as might be expected. Moreover, Guckian et al. solved the solution structure of a duplex containing F opposite A and found that the duplex structure is preserved (*40*). When Seela and co-workers examined the effects of D substitution on A_6-tract curvature, they found that D-substituted duplexes had similar melting temperatures to unsubstituted duplexes (*26*). This suggests that substitution of this analogue does not significantly destabilize the duplex. No structural or stability studies have been published on D,F-substituted duplexes, but McLaughlin and co-workers carried out double analogue substitution experiments with related minor groove modifications (*41*, *42*). When a single modified base pair was introduced into a G−C-rich duplex, no significant decreases in duplex stability were observed. Thus, given these precedents, we expect that our D,F-substituted duplexes are not likely to be structurally perturbed. Furthermore, a number of our modified duplexes do not perturb curvature, which lends added confidence that the results are not due to some kind of anomalous structural or energetic perturbation.

Nielsen and co-workers substituted 2,6-diaminopurine (2,6-DAP) for adenine into an A_5 tract to investigate the role of minor groove width on A-tract curvature (*27*). This analogue introduces an amino group into the minor groove, increasing its width and disrupting the spine of hydration (*43*, *44*). This substitution did result in decreased curvature; however, I_5 (inosine) tracts, which also have a narrow minor groove width (much like that in an A_5 tract), are not curved. Thus, the authors concluded that a narrow minor groove is not sufficient to cause A-tract curvature. Instead, they concluded that their results support a junction-type model (*1*). Seela and Grein also concluded that their results with 3-deazaadenine support the junction model because of the larger effect observed with analogue substitution at the 3′ end. Qualitatively, our results with analogue D are consistent with those of Seela and Grein, and by the same arguments, our results might also be consistent with the junction model. However, a number of our observations are difficult to explain by the junction model alone. First, the effects of D are strongest not at the junction but with one residue removed. Second, it is unlikely that D would alter stacking energetics significantly relative to unmodified A. Diekmann and co-workers found that to preserve stacking, A−T base pairs fold into the minor groove to compensate for the exocyclic amino groups at position 6 of the adenines (i.e., in the major groove) (*45*). The presence of the exocyclic amino group at position 6 and a lack of substitution at position 2 (i.e., in the minor groove) are intrinsic to this interaction. In D, the exocyclic amino group at position 6 is still present, position 2 remains unsubstituted, and the nitrogen at position 3 is substituted for carbon, a very small perturbation unlikely to alter stacking significantly. Finally, the strongest (apparent) minor groove effect in the T-rich strand is far from the 3′ junction of the A tract. Thus, we conclude that most of the present effects are better explained by minor groove electrostatic interactions rather than by a junction stacking effect. In Koo and Crothers' junction model, it is the strong stacking ability of adenine at the junction between A tract and normal DNA that drives the larger 3′ end A-tract curvature (*25*, *29*). In a solution structure of an A_6 tract by Lu and co-workers, the A residues demonstrated increasingly negative inclination from the middle of the A tract to its 3′ end (*4*). We observe only small effects on substitution of the T or A at the 3′ terminus of the tract, while large effects are seen remote from this site, where the junction is unlikely to be affected. Thus, the present data suggest that the junction effect, if real, may be relatively small.

The cation model of A-tract curvature stipulates that cation localization in the minor groove reduces phosphate repulsions between the two strands of duplex DNA, allowing the DNA to collapse or bend in that region. Feigon and co-workers found that Mn^{2+} localized at the first ApA step at the 5′ end of an A_5 tract while ammonium localized near the third and fourth adenines of an A_5 tract. Given that we did not see effects from D2 substitution comparable to those seen with F2 substitution, and assuming that cation localization is occurring around A2 and T2, we conclude that cation localization may occur largely at thymine O2 at the upstream

end of the tract. Likewise, at the downstream portion of the tract, we observe a strong effect of D4 substitution and only a weak effect at the corresponding F4. Thus, it appears that there is a second site of strong interaction, this time with A4 in the fourth base pair of the A_5 tract. The curvature is removed almost completely by the double D4,F2 substitution, and the residual bend is less than that for a single D4 or F2 substitution. This suggests that there are important and at least partially separate interactions at both of those positions.

The current data have now allowed us to probe electrostatic effects along the full length of the minor groove and on both strands of the groove. More data will be needed to assess the relative importance of cation binding and solvation and to explore the effects of different cations on curvature.

SUPPORTING INFORMATION AVAILABLE

Autoradiograms of representative PAGEs and plots for the helical repeat determination and the curvature analyses. This material is available free of charge via the Internet at http://pubs.acs.org.

REFERENCES

1. Koo, H.-S., Wu, H.-M., and Crothers, D. M. (1986) *Nature 320*, 501−506.
2. Burkhoff, A. M., and Tullius, T. D. (1987) *Cell 48*, 935−943.
3. Nelson, H. C. M., Finch, J. T., Bonaventura, F. L., and Klug, A. (1987) *Nature 330*, 221−226.
4. MacDonald, D., Herbert, K., Zhang, X., Polgruto, T., and Lu, P. (2001) *J. Mol. Biol. 306*, 1081−1098.
5. Trifonov, E. N., and Sussman, J. L. (1980) *Proc. Natl Acad. Sci. U.S.A. 77*, 3816−3820.
6. Wu, H.-M., and Crothers, D. M. (1984) *Nature 308*, 509−513.
7. Shui, X., McFail-Isom, L., Hu, G. G., and Williams, L. D. (1998) *Biochemistry 37*, 8341−8355.
8. Shui, X., Sines, C. C., McFail-Isom, L., VanDerveer, D., and Williams, L. D. (1998) *Biochemistry 37*, 16877−16887.
9. Kruger-Woods, K., McFail-Isom, L., Sines, C. C., Howerton, S. B., Stephens, R. K., and Williams, L. D. (2000) *J. Am. Chem. Soc. 122*, 1546−1547.
10. Sines, C. C., McFail-Isom, L., Howerton, S. B., VanDerveer, D., and Williams, L. D. (2000) *J. Am. Chem. Soc. 122*, 11048−11056.
11. Howerton, S. B., Sines, C. C., VanDerveer, D., and Williams, L. D. (2001) *Biochemistry 40*, 10023−10031.
12. Hud, N. V., and Feigon, J. (1997) *J. Am. Chem. Soc. 119*, 5756−5757.
13. Hud, N. V., Sklenar, V., and Feigon, J. (1999) *J. Mol. Biol. 286*, 651−660.
14. Hud, N. V., and Feigon, J. (2002) *Biochemistry 41*, 9900−9910.
15. Young, M. A., Jayaram, B., and Beveridge, D. L. (1997) *J. Am. Chem. Soc. 119*, 59−69.
16. Young, M. A., and Beveridge, D. L. (1998) *J. Mol. Biol. 281*, 675−687.
17. McConnell, K. J., and Beveridge, D. L. (2000) *J. Mol. Biol. 304*, 803−820.
18. Hamelberg, D., McFail-Isom, L., Williams, L. D., and Wilson, W. D. (2000) *J. Am. Chem. Soc. 122*, 10513−10520.
19. Hamelberg, D., Williams, L. D., and Wilson, W. D. (2002) *Nucleic Acids Res. 30*, 3615−3623.
20. Strauss, J. K., and Maher, L. J., III (1994) *Science 266*, 1829−1834.
21. Strauss, J. K., Roberts, C., Nelson, M. G., Switzer, C., and Maher, L. J., III (1996) *Proc. Natl. Acad. Sci. U.S.A. 93*, 9515−9520.
22. Strauss-Soukoup, J. K., Vaghefi, M. M., Hogrefe, R. I., and Maher, L. J., III (1997) *Biochemistry 36*, 8692−8698.
23. Hardwidge, P. R., Lee, D.-K., Prakash, T. P., Iglesias, B., Den, R. B., Switzer, C., and Maher, L. J., III (2001) *Chem. Biol. 8*, 967−980.
24. Hud, N. V., and Plavec, J. (2003) *Biopolymers 69*, 144−158.
25. Diekmann, S., Mazzarelli, J. M., McLaughlin, L. W., von Kitzing, E., and Travers, A. A. (1992) *J. Mol. Biol. 225*, 729−738.
26. Seela, F., and Grein, T. (1992) *Nucleic Acids Res. 20*, 2297−2306.
27. Mollegaard, N. E., Bailly, C., Waring, M. J., and Nielsen, P. E. (1997) *Nucleic Acids Res. 25*, 3497−3502.
28. Maki, A., Brownewell, F. E., Lu, D., and Kool, E. T. (2003) *Nucleic Acids Res. 31*, 1059−1066.
29. Koo, H.-S., and Crothers, D. M. (1987) *Biochemistry 26*, 3745−3748.
30. Mizuno, Y., and Saito, T. I. K. (1964) *Chem. Pharm. Bull. 12*, 866−872.
31. Seela, F., Rosemeyer, H., and Fischer, S. (1990) *Helv. Chem. Acta 73*, 1602−1611.
32. Takeshita, M., Chang, C.-N., Johnson, F., Will, S., and Grollman, A. P. (1960) *J. Biol. Chem. 262*, 10171−10179.
33. Serafinowski, P. (1990) *Synthesis* 757−760.
34. Ross, E. D., Den, R. B., Hardwidge, P. R., and Maher, L. J., III (1999) *Nucleic Acids Res. 27*, 4135−4142.
35. Crothers, D. M., and Drak, J. (1992) *Methods Enzymol. 212*, 46−71.
36. Shatzky-Schwartz, M., Arbuckle, N. D., Eisenstein, M., Rabinovich, D., Bareket-Samish, A., Haran, T. E., Luisi, B. F., and Shakked, Z. (1997) *J. Mol. Biol. 267*, 595−623.
37. Ulanovsky, L., Bodner, M., Trifonov, E. N., and Choder, M. (1986) *Proc. Natl. Acad. Sci. U.S.A. 83*, 862−866.
38. Hardwidge, P. R., Den, R. B., Ross, E. D., and Maher, L. J., III (2000) *J. Biomol. Struct. Dyn. 18*, 219−230.
39. Schweitzer, B. A., and Kool, E. T. (1995) *J. Am. Chem. Soc. 117*, 1863−1872.
40. Guckian, K. M., Krugh, T. R., and Kool, E. T. (1998) *Nat. Struct. Biol. 5*, 954−959.
41. Lan, T., and McLaughlin, L. W. (2000) *J. Am. Chem. Soc. 122*, 6512−6513.
42. Lan, T., and McLaughlin, L. W. (2001) *Biochemistry 40*, 968−976.
43. Bailly, C., Mollegaard, N. E., Nielsen, P. E., and Waring, M. J. (1995) *EMBO J. 14*, 2121−2131.
44. Howard, F. B., Chen, C.-w., Cohen, J. S., and Miles, H. T. (1984) *Biochem. Biophys. Res. Commun. 118*, 848−853.
45. Diekmann, S., von Kitzing, E., McLaughlin, L. W., Ott, J., and Eckstein, F. (1987) *Proc. Natl. Acad. Sci. U.S.A. 84*, 8257−8261.

BI035340M